

Electronic Supplementary Information

Bent Ligand-Directed Assembly and Adsorption Property Modulation of Pseudo-tetrahedral polyoxometalate–organic cages

Meng-Yu Li,^a Ke-Wei Tong,^c Li Zhang,^a Ming-Hua Lu,^a Abudula,^a Bai-Qiao Song,^d
Zun-Qi Liu,^{*ab} Peng Yang^{*c} and Yan-Hu Wang^{*ab}

- a** College of Chemistry and Chemical Engineering
Xinjiang Agricultural University, Urumqi 830052, China
- b** Xinjiang Key Laboratory for High Value Utilization of Agricultural and Livestock
By-products, Urumqi 830052, Xinjiang, China.
E-mail: 19900222wyh@163.com, lzq@xjau.edu.cn
- c** College of Chemistry and Chemical Engineering
Advanced Catalytic Engineering Research Center of the Ministry of Education
Hunan University, Changsha 410082, China
- d** College of Materials and Chemistry & Chemical Engineering
Chengdu University of Technology, Chengdu 610059, China.

Table of Contents (12 pages)

1. Experimental Details	S3
2. Synthesis of Compounds	S4
3. Characterization on Compounds and Ligands	S5
4. Iodine adsorption experiment	S12
5. References	S12

1. Experimental Details

1.1 Materials:

Unless otherwise indicated, all chemicals and reagents were purchased from commercial suppliers and used without further purification. The organic ligands used in this work were synthesized according to the published methods with some modifications.

1.2 Physical measurements:

FT-IR. The Fourier transform infrared (FT-IR) spectra were recorded on KBr disk using a Shimadzu IRSpirit-T spectrometer between 400 and 4000 cm^{-1} .

TGA. Thermogravimetric analyses (TGA) were carried out on a TA Instruments SDT Q600 thermobalance with a 100 mL min^{-1} flow of nitrogen; the temperature was ramped from 30 to 800 $^{\circ}\text{C}$ at a rate of 5 $^{\circ}\text{C min}^{-1}$.

Powder XRD. Powder X-ray diffraction (Powder XRD) patterns were obtained using a Bruker D8 ADVANCE diffractometer with Cu $K\alpha$ radiation ($\lambda = 1.54056 \text{ \AA}$).

X-ray Crystallography. Single crystals of the two compounds were mounted in a Hampton cryoloop with light oil to prevent efflorescence. Single-crystal X-ray diffraction data for both compounds were collected at 150 K using a Bruker D8 Venture diffractometer with Cu $K\alpha$ radiation ($\lambda = 1.5406 \text{ \AA}$). The structure was solved with the ShelXT structure solution program using Intrinsic Phasing¹ and refined with the ShelXL refinement package using Least Squares minimization² operated in the OLEX2 interface.³ All non-hydrogen atoms were refined anisotropically. The hydrogen atoms of the organic groups were introduced in geometrically calculated positions. It was not possible to locate all counter cations by X-ray diffraction, probably due to crystallographic disorder, which is a common problem in polyoxometalate crystallography. Thus, the SQUEEZE program⁴ or the Olex2 solvent mask function⁵ were further used to remove the contributions of weak reflections from the whole data. The newly generated hkl data were further used to refine the final crystal data. The resulting formula units were further used throughout the paper. In the Supporting Information, the crystal data and structure refinement for the compound is summarized in Table S1. CCDC-2539869, 2539870 contains the supplementary crystallographic data for this paper. The data can be obtained free of charge from The Cambridge Crystallographic Data Center via www.ccdc.cam.ac.uk/data_request/cif.

2. Synthesis of Compounds

Synthesis of $(\text{TMA})_8\{[\text{V}_6\text{O}_6(\text{OCH}_3)_9(\text{PyPO}_3)]_4(\text{DBTDC})_6\}\cdot 20\text{CH}_3\text{OH}\cdot 13\text{DMF}$ (TMA-P-VMOT-P-1)

0.040 g (0.250 mmol) of VOSO_4 · 0.020 g (0.0657 mmol) of H_2DBTDC and 0.005 g (0.0314 mmol) of 4-PyPO₃H₃ were suspended in a mixed solvent of DMF : MeOH (1.5 : 3 mL) and sonicated for 30 min. The mixture was sealed in a 25 mL Teflon-lined reactor, which was heated at 150 °C for 60 h. Upon cooling to room temperature at a rate of 10 °C·h⁻¹, dark orange block crystals were obtained. Yield: 0.028 g (37.3% based on VOSO_4). FT-IR (2% KBr pellet, ν/cm^{-1}): 3436 (br), 1664 (s), 1604 (s), 1572 (w), 1556 (m), 1486 (m), 1423 (s), 1397 (s), 1304 (m), 1179 (s), 1071 (s), 950 (s), 778 (s), 663 (m), 562 (s), 535 (w), 501 (w).

Synthesis of $(\text{TMA})_8\{[\text{V}_6\text{O}_6(\text{OCH}_3)_9(\text{NH}_2\text{PhAsO}_3)]_4(\text{DBTDC})_6\}\cdot 15\text{CH}_3\text{OH}\cdot 9.5\text{DMF}$ (TMA-P-VMOT-As-1)

0.060 g (0.226 mmol) of $\text{VO}(\text{acac})_2$ · 0.020 g (0.0657 mmol) of H_2DBTDC and 0.007 g (0.0402 mmol) of p-Arsanilic acid were suspended in a mixed solvent of DMF : MeOH (2 : 4 mL) and sonicated for 30 min. The mixture was sealed in a 25 mL Teflon-lined reactor, which was heated at 150 °C for 60 h. Upon cooling to room temperature at a rate of 10 °C·h⁻¹, light orange block crystals were obtained. Yield: 0.022 g (34.6% based on $\text{VO}(\text{acac})_2$). FT-IR (2% KBr pellet, ν/cm^{-1}): 3435 (br), 2922 (w), 2814 (m), 1598 (s), 1553 (w), 1467 (w), 1421 (m), 1393 (s), 1301 (m), 1176 (s), 1135 (s), 1067 (m), 963 (m), 850 (m), 777 (s), 662 (s), 511 (w).

3. Characterization on Compounds and Ligands

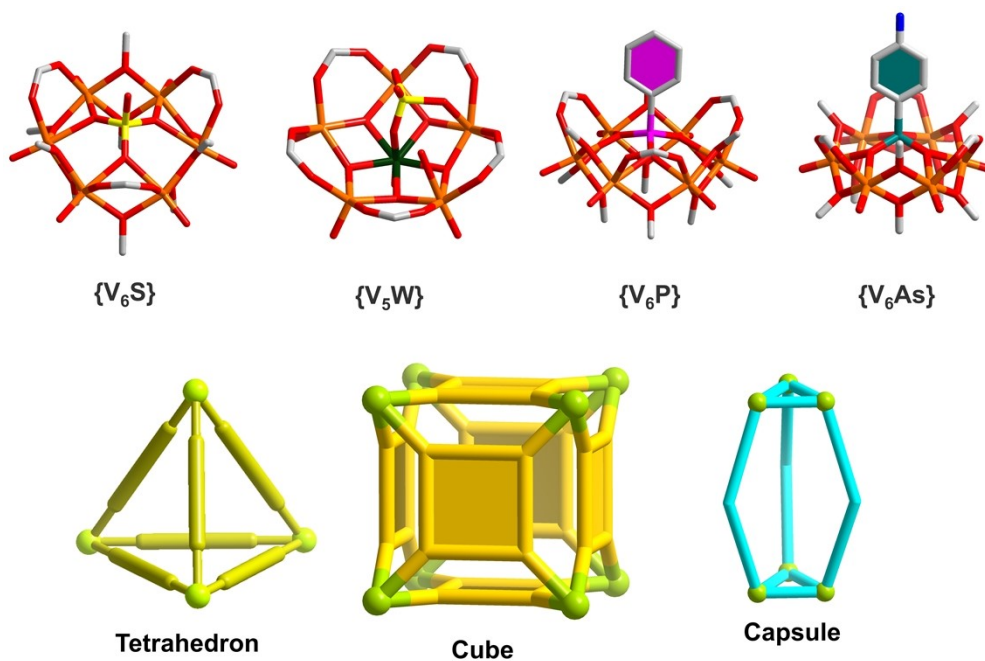


Figure S1. Stick representation of the three-connected ($\{V_6S\}$), ($\{V_6P\}$), ($\{V_6As\}$) and five-connected ($\{V_5W\}$) vertices in POV-MOPs; Ball-and-stick models depicting tetrahedral, cubic, and capsular architectures.

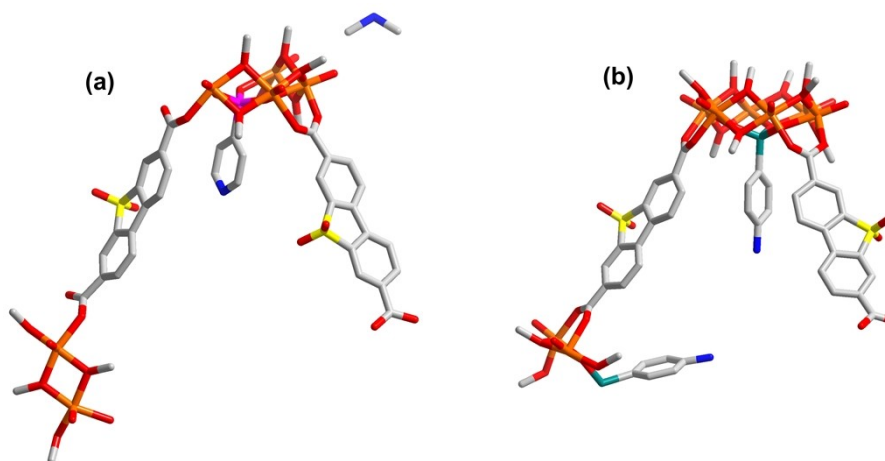


Figure S2. (a, b) The minimum asymmetric units of the as-synthesized compounds.

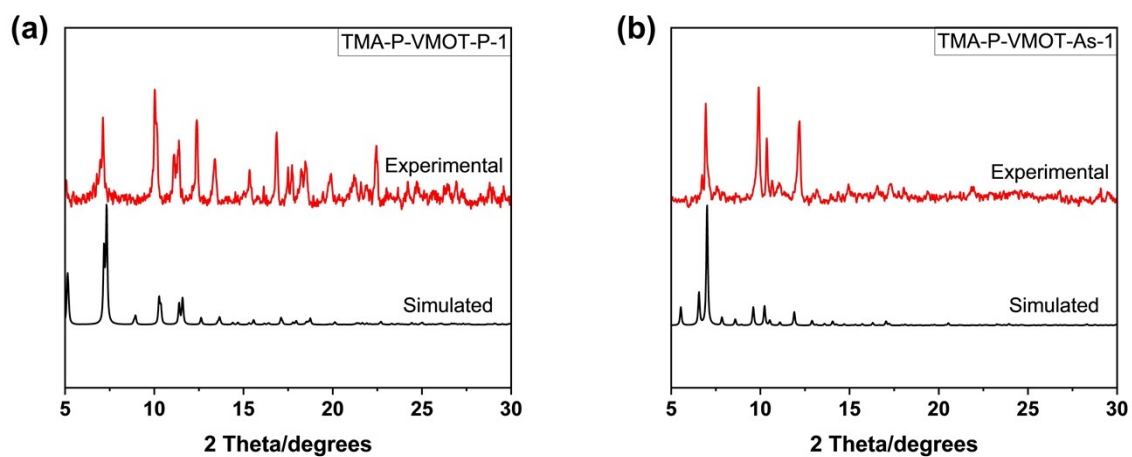


Figure S3. (a, b) Powder XRD patterns of the as-made compounds.

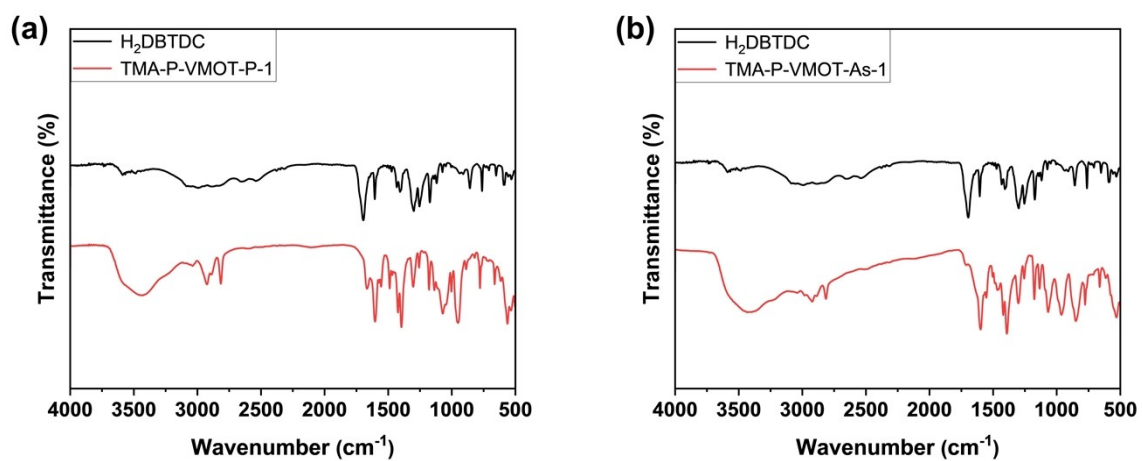


Figure S4. (a, b) FT-IR spectra of the as-made compounds and ligands.

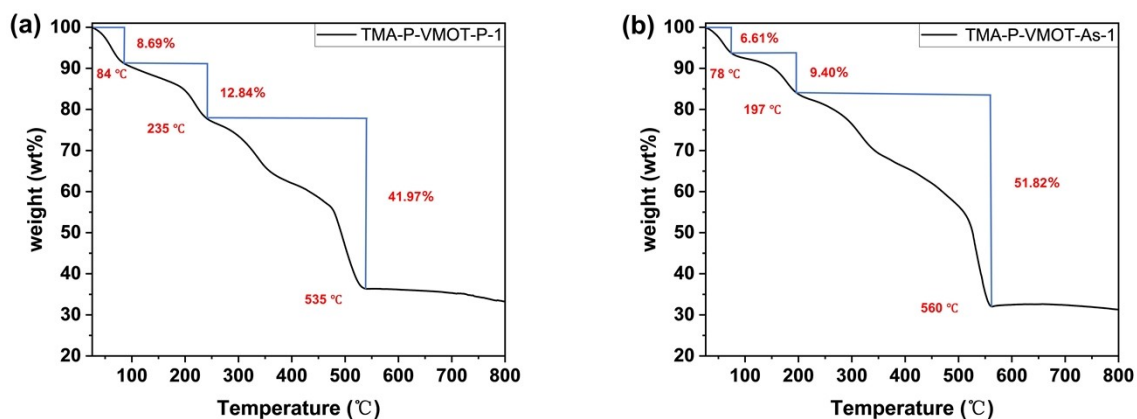


Figure S5. (a) Thermograms of the as-made compounds from 30 to 800 °C under N₂ atmosphere. For **TMA-P-VMOT-P-1**, the first weight loss of 8.69% between 30-83 °C could be attributed to the loss of 20 CH₃OH molecules (calcd. 8.70%). The second weight loss of 12.84% in **TMA-P-VMOT-P-1** from 84 to 235 °C belongs to the release of 13 DMF solvent molecule (calcd. 12.90%). After 235 °C, the backbone of **TMA-P-VMOT-P-1** started to collapse and decomposed completely at 535 °C. (b) Thermograms of the as-made compounds from 30 to 800 °C under N₂ atmosphere. For **TMA-P-VMOT-As-1**, the first weight loss of 6.61% between 30-78 °C could be attributed to the loss of 15 CH₃OH molecules (calcd. 6.70%). The second weight loss of 9.40% in **TMA-P-VMOT-As-1** from 78 to 197 °C belongs to the release of 9.5 DMF solvent molecule (calcd. 9.68%). After 197 °C, the backbone of **TMA-P-VMOT-As-1** started to collapse and decomposed completely at 560 °C.

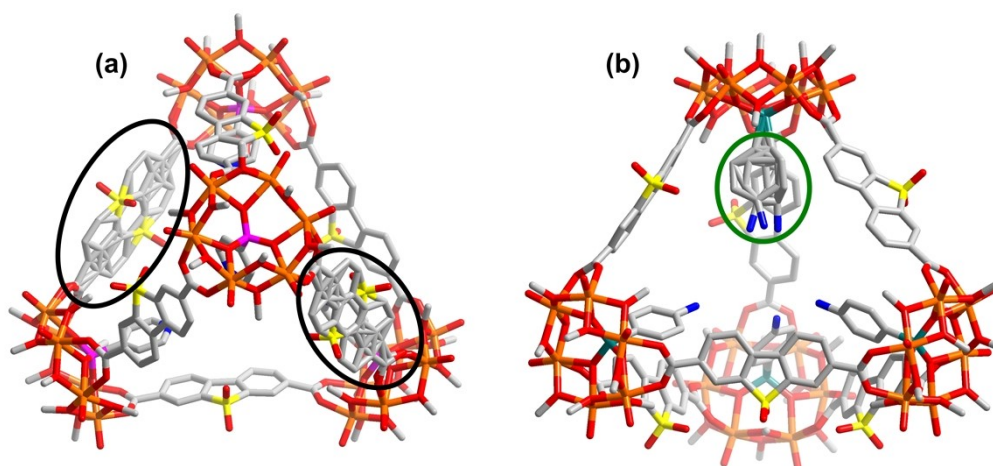


Figure S6. (a, b) Disorder of moieties in the as-prepared compounds.

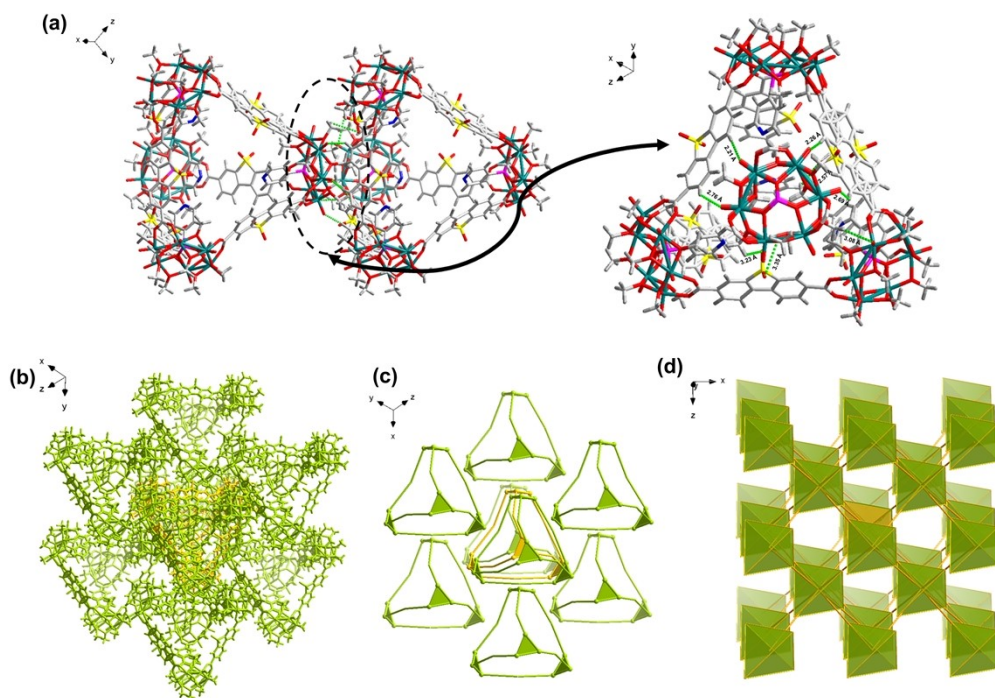


Figure S7. The packing in **P-VMOT-P-1** is directed by a vertex-to-face interaction mode, wherein each cage engages with eight neighbors, resulting in a three-dimensional supramolecular framework.

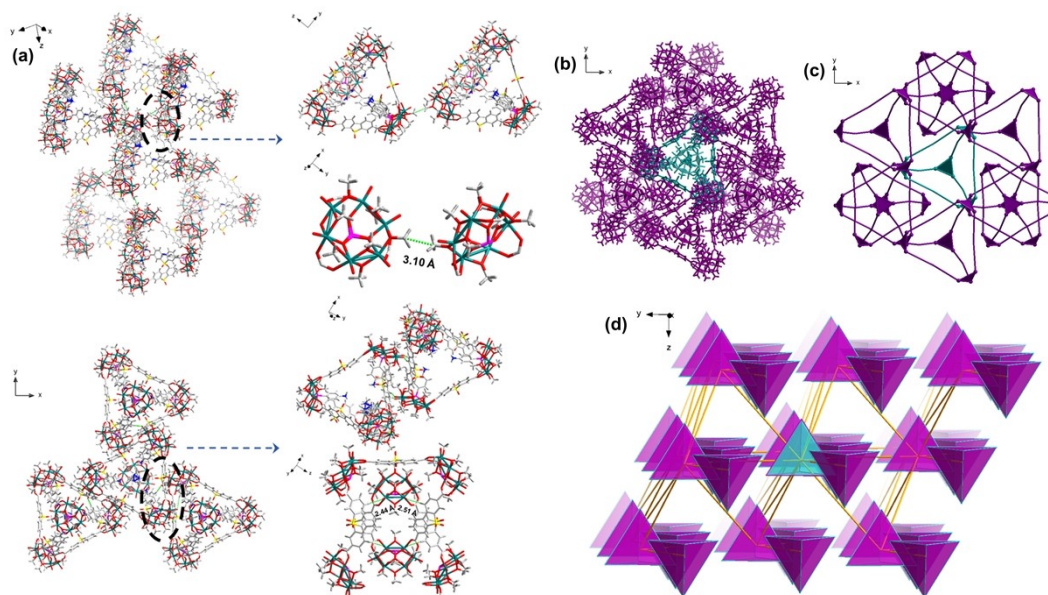


Figure S8. **P-VMOT-As-1** exhibits a distinctive packing mode wherein each pseudo-tetrahedral cage engages with nine neighbors via weak intermolecular forces. Specifically, it connects to three adjacent cages through a shared vertex, to another three via its three triangular faces, and to a final set of three cages through the remaining vertices.

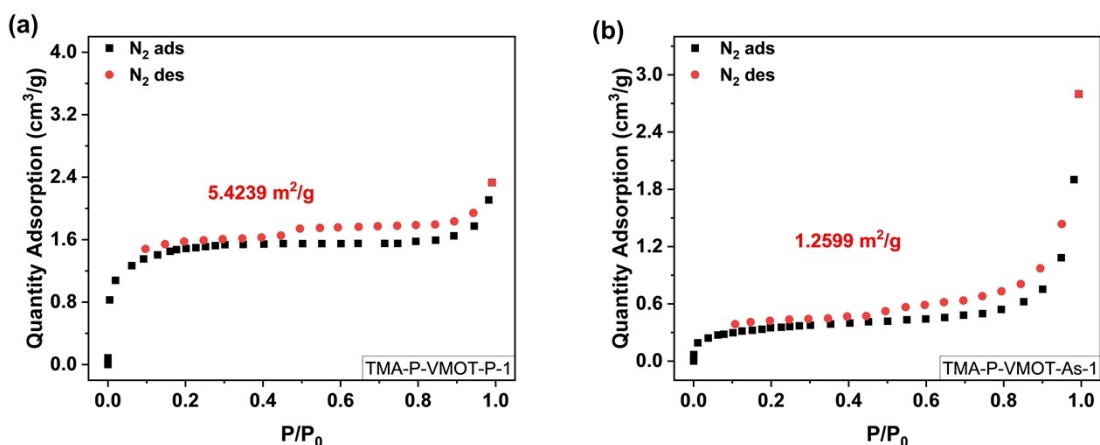


Figure S9 (a, b) N_2 adsorption and desorption isotherms at 77 K for **TMA-P-VMOT-P-1** and **TMA-P-VMOT-As-1**.

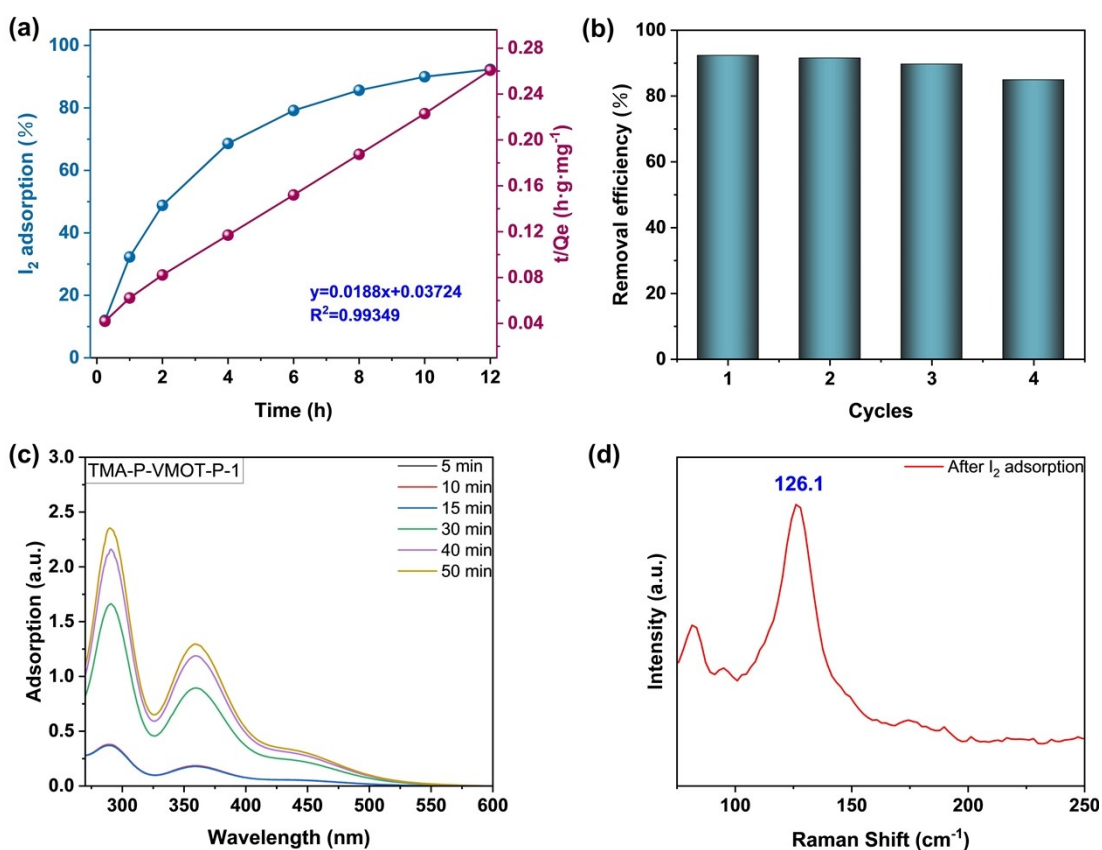


Figure S10. (a) Kinetics of iodine adsorption with **TMA-P-VMOT-P-1**. (b) Evaluation of the adsorbent recyclability: **TMA-P-VMOT-P-1** for Iodine Uptake. (c) Time-dependent iodine release from **TMA-P-VMOT-P-1**. (d) Raman spectroscopic analysis of iodine-adsorbed **TMA-P-VMOT-As-1**.

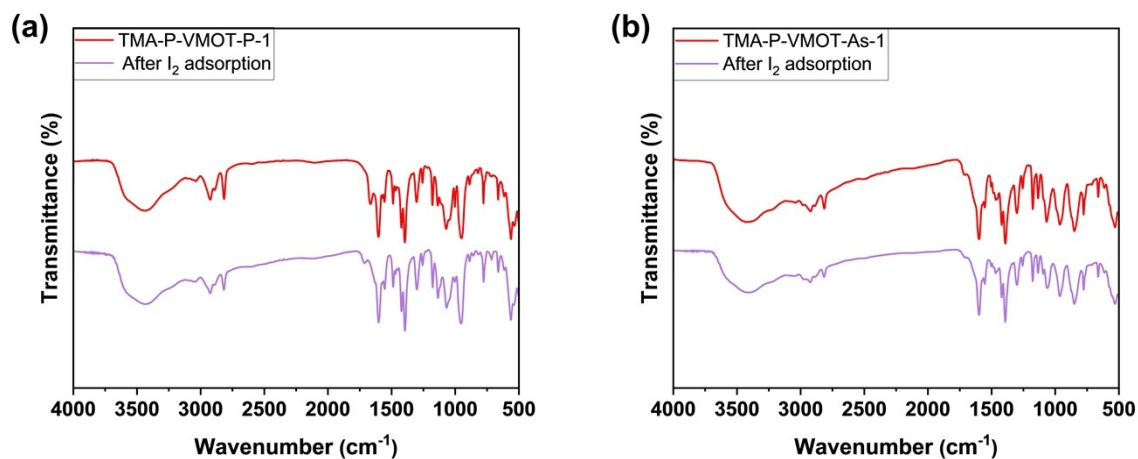


Figure S11. (a, b) FT-IR spectra of **TMA-P-VMOT-P-1** and **TMA-P-VMOT-As-1** before and after iodine adsorption.

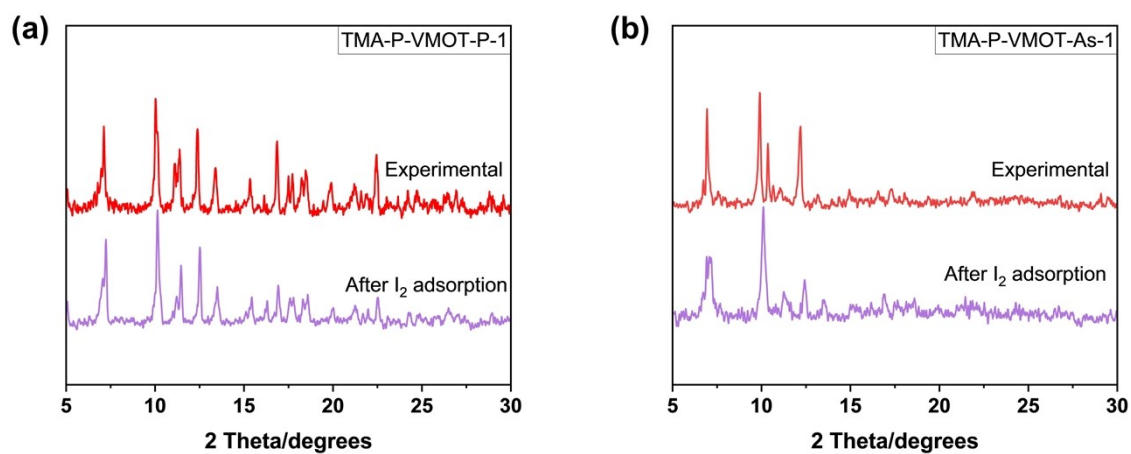


Figure S12. (a, b) Powder XRD patterns of **TMA-P-VMOT-P-1** and **TMA-P-VMOT-As-1** before and after iodine adsorption.

Table S1. Crystal data and structure refinement for the as-made compounds.

Compound	TMA-P-VMOT-P-1	TMA-P-VMOT-As-1
Empirical formula	C ₂₃₁ H ₄₃₅ N ₂₅ P ₄ S ₆ V ₂₄ O ₁₄₁	C _{219.5} H _{390.5} N _{21.5} S ₆ V ₂₄ As ₄ O _{132.5}
Formula weight, g/mol	7357.8905	7165.6870
Crystal system	Tetragonal	Trigonal
Space group	I $\bar{4}$	R $\bar{3}$
a, Å	24.1077(11)	31.8819(4)
b, Å	24.1077(11)	31.8819(4)
c, Å	24.5893(18)	61.6528(16)
α , °	90	90
β , °	90	90
γ , °	90	120
Volume, Å ³	14290.8(17)	54271(2)
Z	2	6
Dcalc, g/cm ³	1.235	0.995
Absorption coefficient, mm ⁻¹	7.510	6.166
F(000)	5372	16283
Theta range for data collection, °	5.13 to 88.96	3.51 to 100.86
Completeness to Θ max	97.3 %	99.9 %
Index ranges	-21 ≤ h ≤ 20 -18 ≤ k ≤ 18 -21 ≤ l ≤ 22	-31 ≤ h ≤ 31 -31 ≤ k ≤ 29 -61 ≤ l ≤ 61
Reflections collected	23812	114878
Independent reflections	5266	12638
R(int)	0.1115	0.2108
Absorption correction	Semi-empirical from equivalents	Semi-empirical from equivalents
Data / restraints / parameters	5266 / 944 / 738	12638 / 214 / 861
Goodness-of-fit on F ²	0.912	1.128
R ₁ , ^[a] wR ₂ ^[b] (I > 2σ(I))	R ₁ = 0.0547 wR ₂ = 0.1264	R ₁ = 0.1004 wR ₂ = 0.3078
R ₁ , ^[a] wR ₂ ^[b] (all data)	R ₁ = 0.1072 wR ₂ = 0.1392	R ₁ = 0.1495 wR ₂ = 0.3478
Largest diff. peak and hole, e/Å ³	0.28 and -0.24	1.25 and -1.83

^[a] $R_1 = \sum ||F_o| - |F_c|| / \sum |F_o|$. ^[b] $wR_2 = [\sum w(F_o^2 - F_c^2)^2 / \sum w(F_o^2)^2]^{1/2}$.

Table S2. BVS values for {V₆P} and {V₆As} of the as-made compounds.

{V ₆ P}	BVS value	{V ₆ As}	BVS value
V1	4.389	V1	4.242
V2	4.355	V2	4.206
V3	4.337	V3	4.034
V4	4.216	V4	4.000
V5	4.643	V5	4.256
V6	4.195	V6	4.345
		V7	4.103
		V8	4.148

Table S3. The data for the lengths and angles of the as-made compounds.

Lengths / Angles	P-VMOT-P-1	P-VMOT-As-1
θ1	161.27°	169.12°
θ2	158.00°	169.12°
θ3	156.17°	169.12°
θ4	161.27°	166.13°
θ5	158.00°	166.13°
θ6	156.17°	165.30°

Table S4. The data for the lengths and angles of the as-made compounds.

Lengths / Angles	P-VMOT-P-1	P-VMOT-As-1
a	15.88 Å	15.80 Å
b	15.88 Å	15.69 Å
c	16.10 Å	16.14 Å
α	60.91°	61.71
β	59.55°	59.51
γ	59.54°	58.78

4. Iodine adsorption experiment

Iodine adsorption in n-hexane. The equimolar (0.005 mmol) freshly prepared crystals of the selected compounds were immersed in 3 mL of I₂/n-hexane solution with a concentration of 2 mmol·L⁻¹, respectively. Then the supernatant monitored periodically at room temperature using UV-vis spectrophotometer.

Iodine Removal Efficiency. The removal efficiency was calculated by using the following equation

$$\text{Removal (\%)} = (C_i - C_{e(\text{or } t)}) / C_i * 100$$

where C_i is the initial concentration of I₂ in n-hexane (mg/L) and C_e is the concentration at equilibrium (mg/L).

References

- [1] G. M. Sheldrick, Crystal structure refinement with SHELXL. *Acta Cryst. C*, **2015**, C71, 3–8.
- [2] G. M. Sheldrick, A short history of SHELX. *Acta Cryst.* **2008**, A64, 112–122.
- [3] O. V. Dolomanov, L. J. Bourhis, R. J. J. A. K. Gildea, Howard, H. Puschmann, OLEX2: a complete structure solution, refinement and analysis program. *J. Appl. Cryst.* **2009**, 42, 339–341.
- [4] A. L. Spek, Crystal structure refinement with SHELXL. *Acta Cryst.* **2015**, C71, 9–18.
- [5] B. Rees, L. Jenner, M. Yusupov, Bulk-solvent correction in large macromolecular structures. *Acta Cryst. D*. **2005**, 61, 1299-1301.